European Journal of Medicinal Chemistry 63 (2013) 57–63

Contents lists available at SciVerse ScienceDirect

European Journal of Medicinal Chemistry

journal homepage: http://www.elsevier.com/locate/ejmech

Short communication

Microwave-assisted synthesis of arene ruthenium(II) complexes that induce S-phase arrest in cancer cells by DNA damage-mediated p53 phosphorylation

Qiong Wu [a,1], Cundong Fan [b,1], Tianfeng Chen [b,**], Chaoran Liu [b], Wenjie Mei [a,b,*], Sidong Chen [c], Baoguo Wang [c], Yunyun Chen [d], Wenjie Zheng [b,**]

[a] School of Pharmacy, Guangdong Pharmaceutical University, Guangzhou, China
[b] Department of Chemistry, Jinan University, Guangzhou, China
[c] Key Laboratory of Molecular Epidemiology, Guangdong Pharmaceutical University, Guangzhou, China
[d] School of Pharmacy, Sun Yat-sen University, Guangzhou, China

ARTICLE INFO

Article history:
Received 11 October 2012
Received in revised form
25 January 2013
Accepted 30 January 2013
Available online 8 February 2013

Keywords:
Arene ruthenium complexes
Microwave assisted synthesis
S-Phase arrest
DNA damage

ABSTRACT

A series of arene ruthenium(II) complexes coordinated by phenanthroimidazole derivates, $[(C_6H_6)Ru(L)Cl]Cl\cdot 2H_2O$ (**1b** L = IP, **2b** L = *p*-NMe_2PIP, **3b** L = *p*-MeOPIP, **4b** L = *p*-HOPIP, **5b** L = *p*-COOHPIP, **6b** L = *p*-CF_3PIP, **7b** L = *p*-BrPIP) have been synthesized in yields of 89–92% under microwave irradiation in 30 min, and the crystal structure of **1b** by XRD gives a typical "piano stool" conformation. The antitumor activity of these complexes against various tumor cells have been evaluated by MTT assay, and the results show that this type of arene Ru(II) complexes exhibit acceptable inhibitory effect against all of these tumor cells, especially osteosarcoma MG-63 cells, but with low toxicity toward HK-2 human normal cells. Studies on the mechanism revealed that cell cycle arrest at S-phase in MG-63 cells induced by the arene Ru(II) complex **2b**, which was confirmed by the increase in the percentage of cells at S-phase and down-regulator of cyclin A. The further studies by Comet assay at single cell level indicated that DNA damage in MG-63 cells was triggered by **2b**, following with the up-regulation of phosphorylated p53 and histone. The studies by spectroscopy *in vitro* also indicate that **2b** bind to DNA molecule by intercalative mode to disturb the bio-function of tumor cells. In conclusion, the synthetic arene Ru(II) complexes could serve as novel p53 activator with potential application in cancer chemotherapy.

1. Introduction

Due to the unavoidable high toxicity, drug resistance and severe side effects of platinum-based anticancer drugs [1,2], ruthenium(II) complexes, especially arene ruthenium(II) complexes have been considered as one of the most promising alternatives owing to their low toxicity, high antitumor activity and strong DNA-binding affinity [3–5]. DNA has long been considered as a common target for antitumor drugs, such as cisplatin, doxorubicin, 5-fluorouracil and paclitaxel which exhibit their therapeutic effects by bonding to DNA molecules [6,7], and there are a large number of evidence indicated that arene Ru(II) complexes can bind to disturb the replication of DNA [8–12]. For example, Sadler et al. indicated that arene Ru(II) complex $[(\eta^6\text{-arene})Ru^{II}(en)Cl]^+$, which exhibit great inhibitory activity against various human tumor cells, can unwind the double strand helix of DNA by forming monofunctional adducts with DNA in intercalative mode [13,14].

In recently, Dyson et al. elucidated that RAPTA-C-induced DNA damage was observed for EAC cells, following the arrest of cell cycle in G2/M phase, as the results the cells proliferation was suppressed [15]. It was worth to indicate that the half-life and transcriptional activity of p53, which are in the central region of the protein responsible for DNA binding [16], are increased in response to the treatment of RAPTA-C [17–20]. It's also reported that up-regulate p53 expression was also observed in apoptosis induced by DW1/2 against melanoma cells [21]. Furthermore, cell cycle arrest in G1 phase through p53-depended and p53-independed mechanism also reported for arene ruthenium-derived compounds (RDCs) [22]. However, there is still little information focused on the S-phase cell cycle arrest through DNA damage-mediated p53 phosphorylation induced by arene ruthenium complexes.

In the present study, a series of arene Ru(II) complexes coordinated by phenanthroimidazole derivatives (Scheme 1) have been

* Corresponding author. School of Pharmacy, Guangdong Pharmaceutical University, Guangzhou, China. Tel./fax: +86 20 39352129.
** Corresponding authors.
E-mail address: wenjiemei@126.com (W. Mei).
[1] These authors contributed equally to the work.

0223-5234/$ – see front matter © 2013 Elsevier Masson SAS. All rights reserved.
http://dx.doi.org/10.1016/j.ejmech.2013.01.037

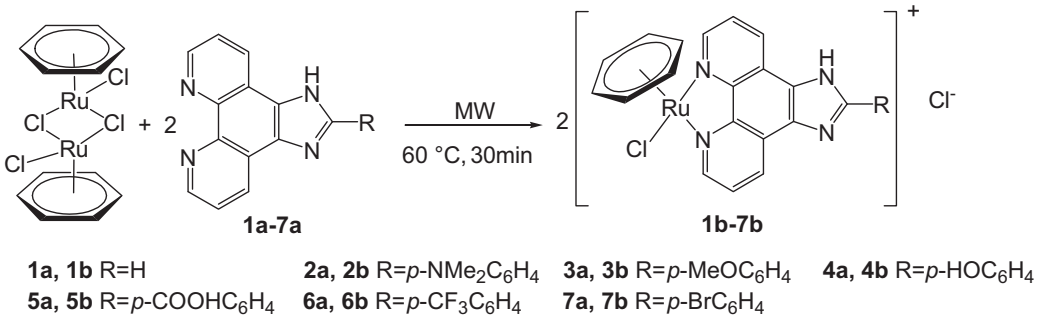

Scheme 1. Microwave-assisted synthesis route for arene Ru (II) complexes.

prepared in high yield under the irradiation of microwave, and the cell cycle arrest in the S-phase through triggering DNA damage by this type of arene ruthenium(II) complexes was investigated.

2. Result and discussion

2.1. Synthesis

The application of microwave irradiation [23] has significantly increased the yield for most of the complexes to about 90%, which were much higher than those of conventional synthesis method (Table 1). Interestingly, complex **5b** that could not be synthesized by liquid phase synthesis method has been produced with yield of 47.5% under the microwave irradiation. Complex **1b** was crystallized and characterized by X-ray diffraction, and the results showed that complex **1b** displayed a typical "piano stool" structure (Fig. 1). As shown in Table 2, the Ru atom was bonded with benzene ring and ligand with an average Ru–C and Ru–N distance of 2.188 (5) and 2.094 (4) Å, respectively. The clear characterization of the chemical structure of the complexes facilitates the understanding of their anticancer mechanisms [24].

2.2. Biological activity

The *in vitro* anticancer activities of the Ru complexes were screened against a series of human cancer cell lines by MTT assay after a 72 h treatment (Table 3). The results indicate that the antiproliferative effects of the complexes were cell-line specific. The most active complex, **2b**, with $-p$-$NMe_2C_6H_4$ group on R position, displayed a broad spectrum growth inhibition against several cancer cells, with IC_{50} value lower than those of other Ru complexes. MG-63 human osteosarcoma cells were sensitive to complex **2b** with IC_{50} value at 36.1 μg/ml. Treatment of MG-63 cells with complex **2b** significantly decreased the cell viability in a dose-dependent manner (Fig. 2A). In the phase-contrast observation (Fig. 2B), the cells treated with complex **2b** for 72 h displayed reduction in cell number, cell shrinkage and loss of cell-to-cell contact. The reduction of cell viability and the change in cell morphology both proved the growth inhibitory effect of Ru(II) complex **2b** on MG-63 cells. Besides this potency, all Ru complexes showed low cytotoxicity toward HK-2 human normal cells, suggesting that the synthetic Ru(II) complexes possess the great selectivity between human cancer and normal cells and display potential application in caner chemotherapy.

Table 1
Yields of Ru complexes by microwave-assisted and conventional synthesis methods.

Complexes	Microwave-assisted			Conventional		
	Temp./°C	Time/h	Yield/%	Temp./°C	Time/h	Yield/%
1b	60	0.5	91.2	60	4	63.5
2b	60	0.5	90.3	60	4	71.4
3b	60	0.5	91.4	60	4	68.8
4b	60	0.5	90.8	60	4	58.7
5b	60	0.5	47.5	60	4	/
6b	60	0.5	91.3	60	4	69.4
7b	60	0.5	89.9	60	4	56.2

2.3. Mechanism studies

Growth inhibition in cancer cells by anticancer drugs could be the result of induction of apoptosis or cell cycle arrest or a combination of these two modes. Therefore, we performed propidium iodide (PI)-flow cytometric analysis to determine action modes of complex **2b**. The results reveal that complex **2b**-induced growth inhibition was mainly caused by cell cycle arrest at S-phase (Fig. 2C). For instance, exposure of MG-63 cells to 5 μg/ml of complex **2b** for 24 h triggered a significant increase of cell proportion at S-phase, accompanied by decrease in the percentage of cells at G2/M phase (Fig. 2D), implying that p53 initiated a S-phase arrest for DNA repair to achieve growth inhibition. Furthermore, MG-63 cells exposed to complex **2b** for 24 h showed dose-dependent decrease in the expression levels of cyclin A (Fig. 2E), which can form a complex with CDK to regulate the progression of cells [25,26]. The down-regulation of cyclin A may disturb the progression of cells at S-phase. Taken together, induction of S-phase arrest by down-regulation of cyclin A could be the major mechanism for cell death induced by complex **2b**.

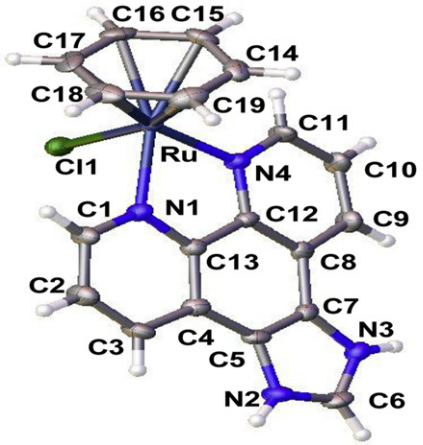

Fig. 1. The ORTEP drawing of arene Ru(II) complex **1b**.

Table 2
Cytotoxic effects of arene Ru(II) complexes on human cancer cell lines.

Complexes	IC_{50} (μg/ml)						
	MG-63	Hela	Neuro-2a	MCF-7	HepG2	LNcap	HK-2
1b	51.5	247.2	82.6	68.1	110.8	78.6	191.7
2b	36.1	88.5	157.2	77.9	>320	176.9	82.8
3b	>320	125.6	138.6	94.3	>320	>320	126.8
4b	>320	112.0	157.3	99.0	175.1	>320	106.4
5b	>320	169.0	>320	>320	295.3	>300	158.0
6b	118.7	178.0	>320	>320	>320	162.5	232.0
7b	91.1	104.0	186.1	114.3	79.5	204.4	129.8

2.4. DNA-binding studies

It is generally accepted that DNA is the target of Ru complexes. To examine synthetic Ru complexes whether induce DNA damage, Western blotting was employed to detect the changes of p53 and histone phosphorylation, two of DNA damage marker, which can be activated in response to DNA damage. As shown in Fig. 3A, MG-63 cells exposed to 5–20 μg/ml of complex **2b** for 24 h showed a noticeable elevation of phosphorylated p53 at Ser15 in a dose-dependent manner, implying that DNA damage was triggered in cells exposed to complex **2b**. Ser139–Histone H2AX, as another DNA damage marker, was also up-regulated in MG-63 cells treated with complex **2b** in a dose-dependent manner. Complex **2b**-induced DNA damage was further confirmed by Comet assay at the single-cell level, which is based on the ability of denatured or cleaved DNA fragments to migrate out of the cell under the influence of an electric field [27]. As shown in Fig. 3B, complex **2b**-induced a remarkable DNA damage in a dose-dependent manner, as evidenced by the increase in tail DNA. Taken together, our results suggest that arene Ru complexes induce S-phase arrest in cancer cells by triggering DNA damage-mediated p53 phosphorylation.

The interaction between the complexes and DNA was confirmed by spectroscopic and viscosity analysis [28]. As shown in Fig. 3C, upon the addition of calf thymus DNA (CT-DNA), obviously hypochromism (18%) and red shift ($\Delta\lambda = 8$ nm) at LMCT (ligand-to-metal charge transition) absorption at 350 nm were observed in the spectra of complex **2b**, with the intrinsic binding constant (K) calculated according to the decay of LMCT absorption to be about 7.78×10^5 M^{-1}. The interaction between complex **2b** and CT-DNA was also confirmed by the fluorescence quenching experiment in EB–DNA system (Fig. 3D). The studies of CD (Fig. 3E) and viscosity analysis (Fig. 3F) showed that complex **2b** may bind to DNA in an intercalating mode, as evidenced by a noticeable decrease in the intensity of the positive CD signal at 275 nm, and increase in the relative viscosity of CT-DNA exposed to complex **2b**.

Table 3
Selected crystallographic data for **1b**.

Identification code	**1b**
Empirical formula	$C_{23}H_{21}N_4O_2RuCl_2$
Formula weight (K)	557.41
Temperature/K	293(2)
Crystal system	Monoclinic
Space group	$C2/c$
a (Å)	21.2331(4)
b (Å)	14.6117(3)
c (Å)	13.6415(3)
α (°)	90.00
β (°)	106.843(2)
γ (°)	90.00
V (Å^3)	4050.74(14)
Z	8
ρ_{calc} mg/mm^3	1.828
m/mm^{-1}	8.959
F(0000)	2248
Reflections collected	8573

3. Conclusions

In conclusion, a series of arene Ru(II) complexes coordinated by phenanthroimidazole derivatives have been synthesized under irradiation of microwave with high yield in 30 min. The synthetic complexes displayed acceptable inhibitory activity against various tumor cells, especially MG-63 cells. Further investigation on the mechanisms revealed that this type of arene Ru(II) complexes could induce S-phase arrest in tumor cells through DNA damage-mediated p53 phosphorylation. Taken together, the synthetic arene Ru(II) complexes could serve as a novel p53 activator with potential application in cancer chemotherapy.

4. Experimental

4.1. Generals

All the chemicals including solvents were obtained from commercial vendors and used as received. The arene Ru(II) complexes were synthesized by Anton Paar GmbH monowave 300. The electronic absorption spectra were recorded on a Shimadzu UV-2550 Spectrophotometer and steady-state emission spectra were recorded on a RF-5301 Fluorescence Spectrophotometer. The ^{1}H NMR spectra were recorded in DMSO-d_6 on BrukerDRX2500 spectrometer and ESI-MS spectra were obtained in methanol on Agilent 1100 ESI-MS system, and the CD spectra were recorded on Jasco J810 Circular Dichroism (CD) spectrophotometer. The X-ray intensity data (0.40 mm × 0.20 mm × 0.10 mm) were collected at 293 (2) K on a Bruker SMART APEX 2K CCD-based X-ray diffractometer equipped with a graphite-monochromated MoKα radiation (λ = 0.71073 Å). The collected frames were processed with the software SHELXTL with 2001 Bruker Analytical X-ray Solutions.

4.2. Synthesis and characterization

4.2.1. Synthesis of *1a*, *2a*, *3a*, *4a*, *5a*, *6a* and *7a*

A solution containing 1,10-phenanthroline-5,6-dione (1.6 mmol, 347 mg), substituted benzaldehyde (1.6 mmol), 20 ml of HAc and NH_4Ac (33 mmol, 2.53 g), was heated at 110 °C under reflux for 4 h. Then, 20 ml of water was added and the pH value was adjusted to 7.0 at room temperature. The solution was filtered and dried in vacuum to obtain a yellow precipitate. The product was purified in a silica gel column by using ethanol as eluent. **1a**: yield 78.4%; mp. 217–219 °C, ESI-MS (in MeOH): m/z: 219.1, ($[M + H]^+$), 438.1, ($[M + 2H]^{2+}$). **2a**: yield 79.5%; mp. 226–228 °C, ESI-MS (in MeOH): m/z: 339.15, ($[M + H]^+$), 678.1, ($[M + 2H]^{2+}$). **3a**: yield 64.4%; mp. 262–265 °C, ESI-MS (in MeOH): m/z: 325.1, ($[M + H]^+$), 650.3, ($[M + 2H]^{2+}$). **4a**: yield 75.7%; mp. 234–236 °C, ESI-MS (in MeOH): m/z: 311.1, ($[M + H]^+$). **5a**: yield 67.1%; mp. 232–235 °C, ESI-MS (in MeOH): m/z: 339.1, ($[M + H]^+$). **6a**: yield 67.7%; mp. 280–283 °C, ESI-MS (in MeOH): m/z: 363.1, ($[M + H]^+$), 726.1, ($[M + 2H]^{2+}$). **7a**: yield 63.4%; mp. 269–273 °C, ESI-MS (in MeOH): m/z: 375.2, ($[M + H]^+$), 750, ($[M + 2H]^{2+}$), 772.8, ($[M + H + Na]^{2+}$).

4.2.2. Synthesis of *1b*, *2b*, *3b*, *4b*, *5b*, *6b* and *7b*

A mixture of $[(C_6H_6)RuCl_2]_2$ (0.1 mmol, 50 mg) and **1a**, **2a**, **3a**, **4a**, **5a**, **6a** and **7a** (0.2 mmol) in 20 ml of dichloromethane was heated in microwave reactor at 60 °C for 30 min. The solvent was removed by rotary evaporation and the residue was dissolved in minimum amounts of methanol and then filtered to remove unreacted ligand to obtain a yellow crude product after recrystallization. **1b**: yield: 91.2%. ESI-MS (in MeOH): m/z 435.1, ($[M - Cl]^+$). UV–visible in

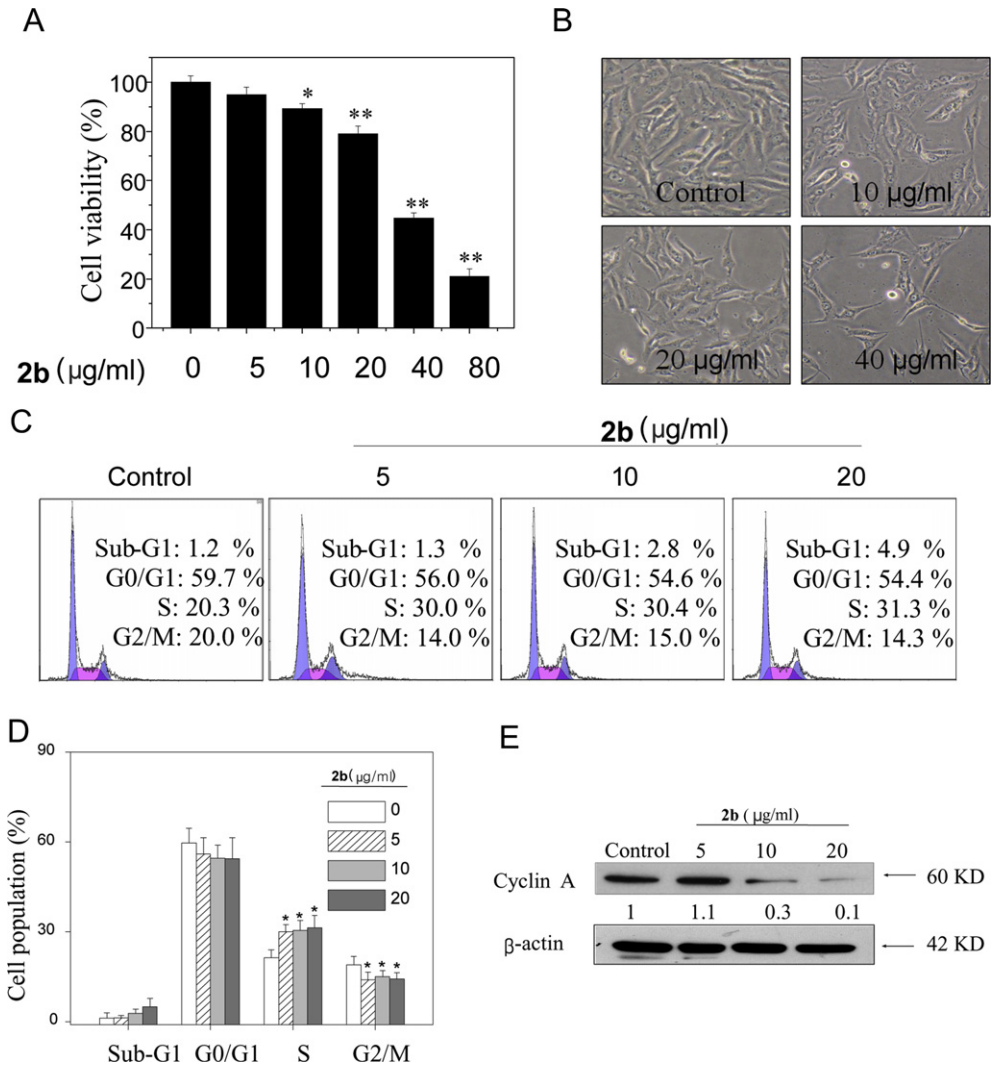

Fig. 2. Complex **2b**-induced S-phase arrest in MG-63 cells. Cells were treated with complex **2b** for 24 h. (A) Cytotoxic effects of complex **2b** on MG-63 cells. (B) Morphological change (magnification, 200×). (C, D) Change in cell cycle distribution. (E) Down-regulation of cyclin A by complex **2b**. All data were obtained from three independent experiments and presented as the means ± SD. $^{*}P < 0.05$ vs untreated control.

MeOH [λ_{max}, nm (ε/M^{-1} cm^{-1})]: 249 (29,585), 295 (20,095). IR (in KBr, ν_{max}/cm^{-1}): 3855.9, 3390.64, 3050.41, 1621.98, 1603.62, 1536.61, 1478.49, 1252.77, 1198.21, 1084.36, 848.13, 811.34, 724.29 cm^{-1}. ^{1}H NMR (DMSO-d_6, δ ppm) δ: 9.84 (d, J = 5.0 Hz, 2H), 9.22 (d, J = 7.9 Hz, 2H), 8.60 (d, J = 8.1 Hz, 2H), 8.09 (dd, J = 8.1, 5.3 Hz, 1H), 6.31 (s, 6H). ^{13}C NMR (126 MHz, DMSO) δ 155.93 (s), 145.19 (s), 144.96 (s), 134.34 (s), 128.00 (s), 88.67 (s). **2b**: yield: 90.3%. ESI-MS (in MeOH): m/z 554.1, ([M − Cl]$^{+}$). UV–visible in MeOH [λ_{max}, nm (ε/M^{-1} cm^{-1})]: 290 (43,780), 342 (38,460). IR (in KBr, ν_{max}/cm^{-1}): 3859.28, 3389.91, 3057.66, 1608.17, 1529.30, 1486.91, 1202.82, 823.99, 812.25, 722.79. ^{1}H NMR (in DMSO-d_6, δ/ppm): 10.20–9.76 (2H, m), 9.60 (2H, t, J = 22.3 Hz), 9.40 (2H, d, J = 8.2 Hz), 9.11 (2H, dd, J = 17.3, 8.0 Hz), 8.57–8.29 (2H, m), 8.28–8.07 (2H, m), 6.91 (2H, t, J = 16.9 Hz), 6.45–6.19 (6H, m). ^{13}C NMR (126 MHz, DMSO) δ 190.31 (s), 151.87 (s), 128.49 (s), 126.17 (s), 116.98 (s), 112.21 (s), 111.50 (s), 87.19 (s). **3b**: yield: 91.4%. ESI-MS (in MeOH): m/z 541.13, ([M − Cl]$^{+}$). UV–visible in MeOH [λ_{max}, nm (ε/M^{-1} cm^{-1})]: 289 (41,520). IR (in KBr, ν_{max}/cm^{-1}): 3862.15, 3423.39, 2987.91, 1610.97, 1524.46, 1483.18, 1255.81, 1181.77, 1066.11, 839.63, 810.66, 722.07. ^{1}H NMR (DMSO-d_6, δ/ppm): 9.96 (dd, J = 5.3, 1.1 Hz, 2H), 8.42 (d, J = 8.6 Hz, 2H), 8.21 (s, 2H), 7.73 (d, J = 8.7 Hz, 2H), 7.37 (s, 2H), 6.33 (s, 6H). ^{13}C NMR (126 MHz, DMSO) δ 162.61 (s), 155.41 (s), 144.84 (s), 134.43 (s), 130.27 (s), 127.64 (s), 116.29 (s), 88.63 (s), 57.30 (s). **4b**: yield: 90.8%. ESI-MS (in MeOH): m/z 527.07, ([M − Cl]$^{+}$). UV–visible in MeOH [λ_{max}, nm (ε/M^{-1} cm^{-1})]: 287 (46,030). IR (in KBr, ν_{max}/cm^{-1}): 3865.69, 3400.23, 3068.44, 1611.12, 1481.83, 1276.56, 1175.75, 842.83, 808.44, 721.33. ^{1}H NMR (in DMSO-d_6, δ/ppm): 9.70 (d, J = 5.2 Hz, 2H), 9.07 (d, J = 7.2 Hz, 2H), 8.76 (d, J = 7.9 Hz, 2H), 8.11 (d, J = 10.6 Hz, 2H), 7.96 (dd, J = 8.2, 5.2 Hz, 2H), 7.37 (s, 2H), 6.28 (s, 6H). ^{13}C NMR (126 MHz, DMSO) δ 161.47 (s), 155.15 (s), 135.98 (s), 129.69 (s), 117.71 (s), 88.65 (s). **5b**: yield: 45.7%. ESI-MS (in MeOH): m/z 555.13, ([M − Cl]$^{+}$). UV–visible in MeOH [λ_{max}, nm (ε/M^{-1} cm^{-1})]: 280 (35,385). IR (in KBr, ν_{max}/cm^{-1}): 3860.42, 3414.54, 3080.94, 1612.23, 1548.55, 1481.39, 1253.06, 1182.67, 1072.72, 838.57, 806.33, 738.21. ^{1}H NMR (DMSO-d_6, δ/ppm): 9.96 (d, J = 4.7 Hz, 2H), 9.20 (dd, J = 31.3, 7.5 Hz, 2H), 8.70 (s, 2H), 8.32–8.06 (m, 2H), 7.37 (s, 2H), 6.32 (s, 6H). ^{13}C NMR (126 MHz, DMSO) δ 156.04 (s), 153.65 (s), 145.34 (s), 131.84 (s), 128.64 (s), 127.96 (s), 88.70 (s). **6b**: yield: 91.3%. ESI-MS (in MeOH): m/z 579.13, ([M − Cl]$^{+}$). UV–visible in MeOH [λ_{max}, nm (ε/M^{-1} cm^{-1})]: 290 (41,885). IR (in KBr, ν_{max}/cm^{-1}): 66.14, 3401.22, 3059.80, 1607.30, 1620.53, 1551.47, 1454.98, 1167.3, 851.02, 810.46, 722.48. ^{1}H NMR (DMSO-d_6, δ ppm): 9.91 (d, J = 4.7 Hz, 2H), 8.31 (t, J = 11.1 Hz, 2H),

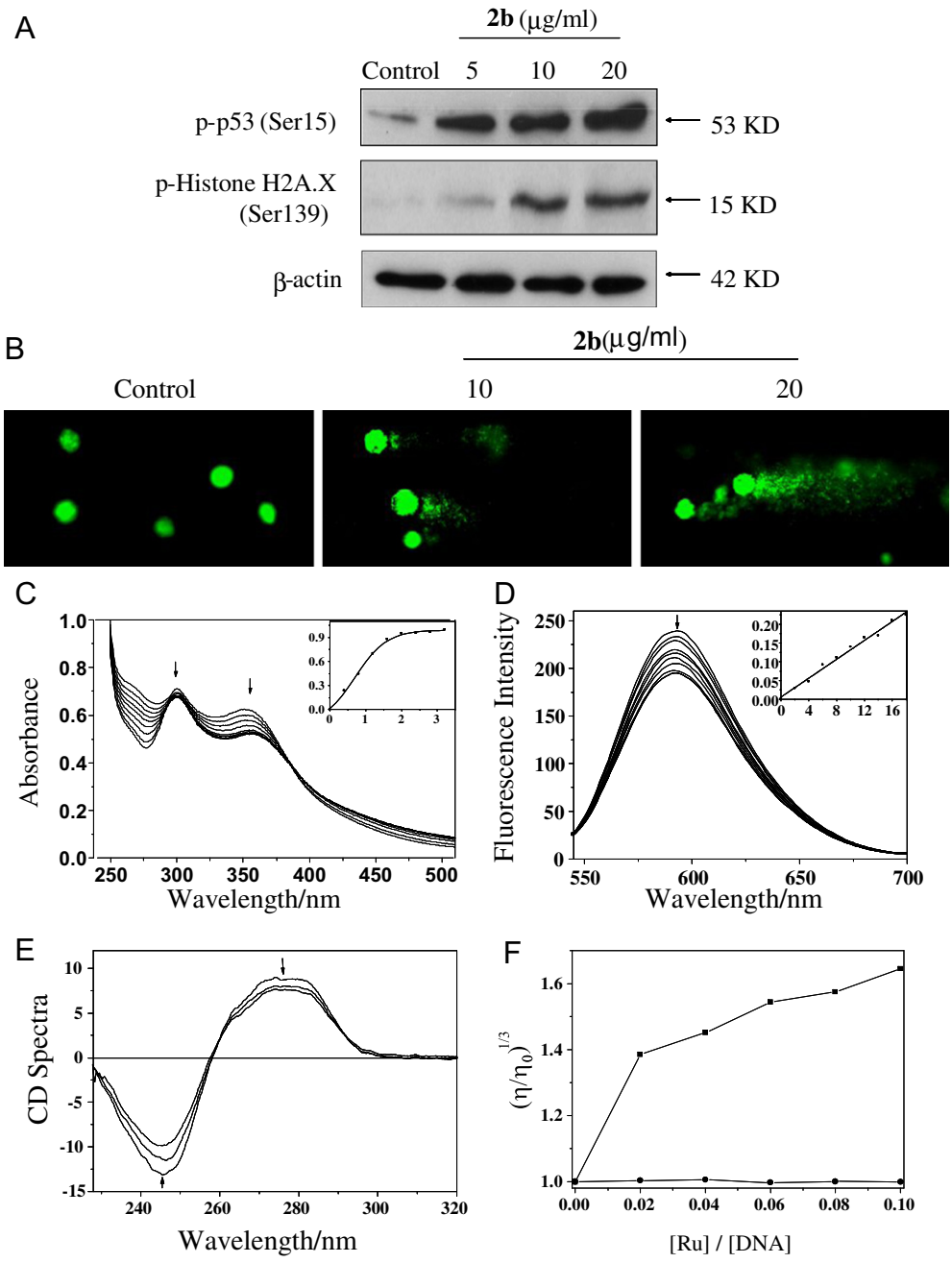

Fig. 3. (A) Effects of complex **2b** on the expression level of phosphorylated p53 and Histone H2A X. (B) DNA damage induced by complex **2b** as examined by Comet assay. Cells were treated for 24 h and the length of tail reflects DNA damage in the cells. (C–F) DNA-binding behavior of complex **2b** with CT-DNA. (C) Absorption spectra of complex **2b** in Tris–HCl buffer upon addition of increasing concentrations of CT-DNA. [Ru] = 20 μM. (D) Emission spectra of EB and CT-DNA in Tris–HCl buffer with addition of complex **2b**. [EB] = 16 μM, [DNA] = 100 μM. (E) CD spectra of CT-DNA with addition of complex **2b**. [DNA] = 300 μM, [Ru] = 2 and 6 μM. (F) Effects of complex **2b** (■) and $[Ru(bpy)_3]^{+}$ (●) on the relative viscosity of CT-DNA.

8.13 (dd, J = 23.8, 15.5 Hz, 2H), 7.37 (s, 2H), 6.98 (d, J = 8.7 Hz, 2H), 6.32 (s, 6H). ^{13}C NMR (126 MHz, DMSO) δ 156.03 (s), 145.39 (s), 129.24 (s), 127.95 (s), 88.70 (s). **7b**: yield: 89.8%. ESI-MS (in MeOH): m/z 590.9, ([M − Cl]$^{+}$). UV–visible in MeOH [λ_{max}, nm (ε/M^{-1} cm^{-1})]: 283 (46,320). IR (in KBr, ν_{max}/cm^{-1}): 3869.75, 3369.99, 3042.42, 1625.14, 1603.67, 1543.71, 1459.87, 1275.97, 1186.24, 1070.50, 722.92. ^{1}H NMR (DMSO-d_6, δ ppm) δ: 9.93 (dd, J = 5.3, 1.1 Hz, 2H), 8.31 (d, J = 8.6 Hz, 2H), 8.18 (dd, J = 8.1, 5.5 Hz, 2H), 7.84 (d, J = 8.6 Hz, 2H), 7.34 (s, 2H), 6.30 (s, 6H). ^{13}C NMR (126 MHz, DMSO) δ 150.45 (s), 133.93 (s), 131.31 (s), 130.17 (s), 127.35 (s), 124.51 (s), 88.59 (s).

4.3. Biochemical approach

4.3.1. MTT assay

Human cancer cell lines, including melanoma A375, hepatocellular carcinoma HepG2 and colorectal adenocarcinoma SW620, were purchased from American Type Culture Collection (ATCC, Manassas, VA). The normal fibroblast Hs68 and kidney HK-2 cells were also obtained from ATCC. All cell lines were maintained in either RPMI-1640 or DMEM media supplemented with fetal bovine serum (10%), penicillin (100 units/ml) and streptomycin (50 units/ml) at 37 °C in CO_2 incubator (95% relative humidity, 5% CO_2). Cell

viability was determined by measuring the ability of cells to transform MTT to a purple formazan dye [29]. Cells were seeded in 96-well tissue culture plates for 24 h. After incubation, 20 μl/well of MTT solution (5 mg/ml phosphate buffered saline) was added and incubated for 5 h. The color intensity of the formazan solution, which reflects the cell growth condition, was measured at 570 nm using a microplate spectrophotometer (SpectroAmax™ 250).

4.3.2. Flow cytometric analysis

The cell cycle distribution was analyzed by flow cytometry as previously described [30]. Treated or untreated cells were trypsinized, washed with PBS and fixed with 75% ethanol overnight at −20 °C. The fixed cells were washed with PBS and stained with propidium iodide (PI) (1.21 mg/ml Tris, 700 U/ml RNase, 50.1 μg/ml PI, pH8.0) for 4 h in darkness. Cell cycle distribution was analyzed using MultiCycle software (Phoenix Flow Systems, San Diego, CA). Apoptotic cells with hypodiploid DNA content were measured by quantifying the sub-G1 peak in the cell cycle pattern.

4.3.3. Western blot analysis

Total cellular proteins were extracted by incubating cells in lysis buffer obtained from Cell Signaling Technology and protein concentrations were determined by BCA assay. SDS-PAGE was done in 10% tricine gels loading equal amount of proteins per lane. After electrophoresis, separated proteins were transferred to nitrocellulose membrane and blocked with 5% non-fat milk in TBST buffer for 1 h. After then, the membranes were incubated with primary antibodies at 1:1000 dilutions in 5% non-fat milk overnight at 4 °C, and then secondary antibodies conjugated with horseradish peroxidase at 1:2000 dilution for 1 h at room temperature. Protein bands were visualized on X-ray film using an enhanced chemiluminescence system (Kodak).

4.3.4. Comet assay

Single-cell gel electrophoresis for detection of DNA damage was performed using the Comet assay reagent kit purchased from Trevigen according to the manufacturer's instructions. DNA was stained with SYBR Green I (Trevigen) and visualized under a fluorescence microscope (Nikon, Eclipse E-600). Fifty cells per slide were selected randomly and their olive tail moments were determined using an image analysis system (Komet 3.1, Kinetics Imaging Ltd., Liverpool) linked to a CCD camera.

4.4. DNA-binding behavior

4.4.1. UV titration

The DNA-binding and cleavage experiments were performed at room temperature. The concentration of the complex (**2b**) solution was 10 μM and CT-DNA was added to a ratio of 6:1 [DNA]/[Ru]. The intrinsic binding constant K of ruthenium(II) complex to DNA was calculated from the following equations [31].

$$(\varepsilon_a - \varepsilon_f)/(\varepsilon_b - \varepsilon_f) = [b - (b^2 - 2K^2C_t[\mathrm{DNA}]/S)]^{1/2}/2KC_t \quad (1)$$

$$b = 1 + KC_t + K[\mathrm{DNA}]/2S \quad (2)$$

4.4.2. Fluorescence quenching

Fluorescence quenching of EB–DNA complex can be used for a compound having an affinity to DNA in spite of its binding mode, and only measures the ability of the compound to affect the EB fluorescence intensities in the EB–DNA complex [32]. According to the quenching curve we can draw a preliminary conclusion that the complex can competitively bind to DNA by replacing EB.

4.4.3. CD spectrum

CD spectral characteristics were compared for CT-DNA in the absence and in the presence of complex **2b**, respectively. Complex **2b** has no intrinsic CD signals, as it is achiral so that any CD signal above 300 nm can be attributed to the interaction of complex with DNA. This increase of decrease was similar to that observed if DNA was under identical conditions modified by cisplatin of ineffective transplatin, respectively [33].

4.4.4. Viscosity

Viscosity test is one of the most effective methods to judge the interaction mode of complexes with DNA. Prepare different concentrations of fixed solution of complex **2b** and DNA in Tris/HCl buffer media, which is [**2b**]/[DNA] = 0, 0.02, 0.04, 0.06, 0.08, 0.1. Before testing, keep them (30 ± 0.1 °C) 1 h in thermostatic water bath. The formula calculated viscosity is: $\eta = (t - t_0)/t_0$. Viscosity curves were obtained by a picture with $(\eta/\eta_0)^{1/3}$ as *Y*-axis and with $r(r = [\mathbf{2b}]/[\mathrm{DNA}])$ as *X*-axis.

Acknowledgments

This work was supported by Natural Science Foundation of China and Guangdong Province, Key Project of Science and Technology Department of Guangdong Province, Science and Technology Planning Project of Guangdong Province, the Fundamental Research Funds for the Central Universities, Program for New Century Excellent Talents in University and the Doctoral Foundation of Ministry of Education of China.

Appendix A. Supplementary data

Supplementary data related to this article can be found at http://dx.doi.org/10.1016/j.ejmech.2013.01.037.

References

[1] M. Markman, Toxicities of the platinum antineoplastic agents, Expert Opin. Drug Saf. 2 (2003) 597–607.
[2] P.C. Bruijnincx, P.J. Sadler, New trends for metal complexes with anticancer activity, Curr. Opin. Chem. Biol. 12 (2008) 197–206.
[3] D. Wesselinova, N. Kaloyanov, G. Dimitrov, Cytotoxicity and effects of 1,10-phenanthroline and 5-amino-1,10-phenanthroline derivatives on some immunocompetent cells, Eur. J. Med. Chem. 44 (2009) 5099–5102.
[4] C. Scolaro, A.B. Chaplin, C.G. Hartinger, A. Bergamo, M. Cocchietto, B.K. Keppler, G. Sava, P.J. Dyson, Tuning the hydrophobicity of ruthenium(II)-arene (RAPTA) drugs to modify uptake, biomolecular interactions and efficacy, Dalton Trans. (2007) 5065–5072.
[5] K.K. Lo, T.K. Lee, Luminescent ruthenium(II) polypyridine biotin complexes: synthesis, characterization, photophysical and electrochemical properties, and avidin-binding studies, Inorg. Chem. 43 (2004) 5275–5282.
[6] P. Govender, A.K. Renfrew, C.M. Clavel, P.J. Dyson, B. Therrien, G.S. Smith, Antiproliferative activity of chelating *N,O*- and *N,N*-ruthenium(II) arene functionalised poly(propyleneimine) dendrimer scaffolds, Dalton Trans. 40 (2011) 1158–1167.
[7] R. Palchaudhuri, P.J. Hergenrother, DNA as a target for anticancer compounds: methods to determine the mode of binding and the mechanism of action, Curr. Opin. Biotechnol. 18 (2007) 497–503.
[8] H.K. Liu, P.J. Sadler, Metal complexes as DNA intercalators, Acc. Chem. Res. 44 (2011) 349–359.
[9] L.J. Ming, Structure and function of metalloantibiotics, Med. Res. Rev. 23 (2003) 697–762.
[10] O. Novakova, J. Kasparkova, V. Bursova, C. Hofr, M. Vojtiskova, H. Chen, P.J. Sadler, V. Brabec, Conformation of DNA modified by monofunctional Ru(II) arene complexes: recognition by DNA binding proteins and repair relationship to cytotoxicity, Chem. Biol. 12 (2005) 121–129.
[11] O. Novakova, J. Malina, T. Suchankova, J. Kasparkova, T. Bugarcic, P.J. Sadler, V. Brabec, Energetics, conformation, and recognition of DNA duplexes modified by monodentate Ru(II) complexes containing terphenyl arenes, Chem. Eur. J. 16 (2010) 5744–5754.
[12] O. Novakova, H. Chen, O. Vrana, A. Rodger, P.J. Sadler, V. Brabec, DNA interactions of monofunctional organometallic ruthenium(II) antitumor complexes in cell-free media, Biochemistry 42 (2003) 11544–11554.

[13] R.E. Morris, R.E. Aird, P.D. Murdoch, H.M. Chen, J. Cummings, N.D. Hughes, S. Parsons, A. Parkin, G. Boyd, D.I. Jodrell, P.J. Sadler, Inhibition of cancer cell growth by ruthenium(II) arene complexes, J. Med. Chem. 44 (2001) 3616–3621.
[14] S.W. Magennis, A. Habtemariam, O. Novakova, J.B. Henry, S. Meier, S. Parsons, I.D.H. Oswald, V. Brabec, P.J. Sadler, Dual triggering of DNA binding and fluorescence via photoactivation of a dinuclear ruthenium(II) arene complex, Inorg. Chem. 46 (2007) 5059–5068.
[15] S. Chatterjee, S. Kundu, A. Bhattacharyya, C.G. Hartinger, P.J. Dyson, The ruthenium(II)-arene compound RAPTA-C induces apoptosis in EAC cells through mitochondrial and p53-JNK pathways, J. Biol. Inorg. Chem. 13 (2008) 1149–1155.
[16] K.H. Vousden, X. Lu, Live or let die: the cell's response to p53, Nat. Rev. Cancer 2 (2002) 594–604.
[17] J.L. Yu, J.W. Rak, B.L. Coomber, D.J. Hicklin, R.S. Kerbel, Effect of p53 status on tumor response to antiangiogenic therapy, Science 295 (2002) 1526–1528.
[18] M.V. Blagosklonny, P53: an ubiquitous target of anticancer drugs, Int. J. Cancer 98 (2002) 161–166.
[19] Y. Liu, R. Hammitt, D.A. Lutterman, L.E. Joyce, R.P. Thummel, C. Turro, Ru(II) complexes of new tridentate ligands: unexpected high yield of sensitized $^1O_2$, Inorg. Chem. 48 (2009) 375–385.
[20] Y. Liu, R. Hammitt, D.A. Lutterman, R.P. Thummel, C. Turro, Marked differences in light-switch behavior of Ru (II) complexes possessing a tridentate DNA intercalating ligand, Inorg. Chem. 46 (2007) 6011–6021.
[21] K.S. Smalley, R. Contractor, N.K. Haass, A.N. Kulp, G.E. Atilla-Gokcumen, D.S. Williams, H. Bregman, K.T. Flaherty, M.S. Soengas, E. Meggers, M. Herlyn, An organometallic protein kinase inhibitor pharmacologically activates p53 and induces apoptosis in human melanoma cells, Cancer Res. 67 (2007) 209–217.
[22] C. Gaiddon, P. Jeannequin, P. Bischoff, M. Pfeffer, C. Sirlin, J.P. Loeffler, J. Pharmacol. Exp. Ther. 315 (2005) 1403–1411.
[23] F.A. Beckford, M. Shaloski Jr., G. Leblanc, J. Thessing, L.C. Lewis-Alleyne, A.A. Holder, L. Li, N.P. Seeram, Microwave synthesis of mixed ligand diimine–thiosemicarbazone complexes of ruthenium(II): biophysical reactivity and cytotoxicity, Dalton Trans. (2009) 10757–10764.
[24] I.W. McNae, K. Fishburne, A. Habtemariam, T.M. Hunter, M. Melchart, F. Wang, M.D. Walkinshaw, P.J. Sadler, Half-sandwich arene ruthenium(II)–enzyme complex, Chem. Commun. (Camb.) (2004) 1786–1787.
[25] Y. Cho, S. Gorina, P.D. Jeffrey, N.P. Pavletich, Crystal structure of a p53 tumor suppressor-DNA complex: understanding tumorigenic mutations, Science 265 (1994) 346–355.
[26] Z. Guo, C. Zhuang, L. Zhu, Y. Zhang, J. Yao, G. Dong, S. Wang, Y. Liu, H. Chen, C. Sheng, Z. Miao, W. Zhang, Structure–activity relationship and antitumor activity of thio-benzodiazepines as p53–MDM2 protein–protein interaction inhibitors, Eur. J. Med. Chem. 56 (2012) 10–16.
[27] D.W. Fairbairn, P.L. Olive, K.L. O'Neill, Heterogeneity in human tumour hypoxic fraction using the comet assay, Mutat. Res. 339 (1995) 37–59.
[28] V. Vajpayee, Y.H. Song, M.H. Lee, H. Kim, M. Wang, P.J. Stang, K.W. Chi, Self-assembled arene-ruthenium-based rectangles for the selective sensing of multi-carboxylate anions, Chem. Eur. J. 17 (2011) 7837–7844.
[29] T. Chen, Y.S. Wong, Selenocystine induces reactive oxygen species-mediated apoptosis in human cancer cells, Biomed. Pharmacother. 63 (2009) 105–113.
[30] T. Chen, Y.S. Wong, Selenocystine induces S-phase arrest and apoptosis in human breast adenocarcinoma MCF-7 cells by modulating ERK and Akt phosphorylation, J. Agric. Food Chem. 56 (2008) 10574–10581.
[31] M.T. Carter, M. Rodriguez, A. Bard, Voltammetric studies of the interaction of metal chelates with DNA. 2. Tris-chelated complexes of cobalt(III) and iron(II) with 1,10-phenanthroline and 2,2′-bipyridine, J. Am. Chem. Soc. 111 (1989) 8901–8911.
[32] W.J. Mei, J. Liu, H. Chao, L.N. Ji, DNA-binding and cleavage studies of a novel porphyrin ruthenium mixed complex $[MPyTPP\text{-}Ru(pip)_2Cl]^+$, Transition Met. Chem. 28 (2003) 852–857.
[33] V. Brabec, V. Kleinwachter, J.L. Butour, N.P. Johnson, Biophysical studies of the modification of DNA by antitumour platinum coordination complexes, Biophys. Chem. 35 (1990) 129–141.